Carbohydrate Polymer Technologies and Applications 7 (2024) 100467

Contents lists available at ScienceDirect

Carbohydrate Polymer Technologies and Applications

journal homepage: www.sciencedirect.com/journal/carbohydrate-polymer-technologies-and-applications

Bio-based composites from bagasse using carbohydrate enriched cross-bonding mechanism: A formaldehyde-free approach

Md. Nazrul Islam [a,*], Afroza Akter Liza [b], Moutusi Dey [a], Atanu Kumar Das [c], Md Omar Faruk [d], Mst Liza Khatun [a], Md Ashaduzzaman [a], Xuedong Xi [e]

[a] Forestry and Wood Technology Discipline, Khulna University, Khulna 9208, Bangladesh
[b] Jiangsu Co-Innovation Center for Efficient Processing and Utilization of Forest Resources and International Innovation Center for Forest Chemicals and Materials, Nanjing Forestry University, Nanjing 210037, China
[c] Department of Forest Biomaterials and Technology, Swedish University of Agricultural Sciences, SE-90183 Umeå, Sweden
[d] Shushilan, Jalil Sharoni, 155 Jalil-Sarani, Khulna 9100, Bangladesh
[e] College of Materials and Chemical Engineering, Southwest Forestry University, 650224 Kunming, China

ARTICLE INFO

Keywords:
Sugarcane bagasse
Bio-based adhesive
Cross-bonded boards
Physical properties
Mechanical properties

ABSTRACT

In this study, cross-bonded self-binding and bone glue-bonded particleboards were manufactured from sugarcane (*Saccharum officinarum* L.) bagasse with different pre-treatments of particles. Six types of panels were manufactured from bagasse particles with and without bone glue. The physical, mechanical, and thermal properties of the panels were examined according to the standards. Fourier Transform Infrared (FTIR) spectroscopy and thermogravimetric analysis (TG) were performed to investigate the changes in the chemical bonds and thermal stability of the fabricated composites, respectively. It was found that cross-bonded bagasse self-binding (T_C) and bone glue-bonded (T_3) panels fabricated from non-boiled bagasse particles showed higher physical and mechanical properties compared to the other types of panels. Non-boiled bagasse particles with bone glue panels showed the highest mechanical properties, i.e., modulus of rupture (MOR = 26.22 MPa), modulus of elasticity (MOE = 4302 MPa), tensile strength = 8.35 MPa, and hardness = 1.72 MPa. T_C and T_3 panels also showed higher thermal stability compared to the other types of panels. A new peak at 3331–3334 cm^{-1} for the N—H stretching vibration in the FTIR analysis represents the presence of bone glue in the cross-bonded particleboards. Thus, this research advances the production of formaldehyde-free bagasse particleboard, introducing the cross-bonding technique and sustainable bone glue.

Introduction

In recent years, the demand for adhesive-bonded composite products has increased substantially worldwide, particularly for housing construction and furniture manufacturing (Baharuddin et al., 2023). The most common types of fossil-based adhesives applied in the wood industry are mostly synthetic adhesives and their related products, including poly (vinyl acetate), epoxy, phenol-formaldehyde, and polyurethane (Islam et al., 2022; Liu et al., 2019). Composite product manufacturing incorporates synthetic adhesives that include hazardous substances such as formaldehyde and volatile organic compounds (VOCs) (Boon et al., 2019). In response to issues relating to health and the environment, different options are being developed by industries (Ferrandez-Villena et al., 2020). Although formaldehyde-based bonding enhances the characteristics of products, it also results in the release of toxic gaseous emissions that have negative effects on the environment and human health (Salthammer et al., 2010; Zhou et al., 2013; Zhang et al., 2015). Many countries have implemented stringent regulations on the release of formaldehyde, which has spurred investigations into alternate possibilities (Boon et al., 2019).

Thus, the development of bio-based adhesives from natural biopolymers, such as protein, starch, lignin, tannin, etc., is of the utmost importance for researchers (Wang et al., 2012; Sulaiman et al., 2018; Islam et al., 2022; Zhang et al., 2023). Bone glue, derived from waste bones, is gaining attention due to its protein content (Islam et al., 2021). The use of self-bonding or binderless particleboards, a technique that does not rely on adhesives, has been proposed by researchers (Boon et al., 2019; Ferrandez-Villena et al., 2020, Vitrone et al., 2021). This

* Corresponding author.
E-mail address: nazrul17@yahoo.com (Md.N. Islam).

https://doi.org/10.1016/j.carpta.2024.100467

Available online 7 March 2024

process depends on lignocellulosic materials' self-bonding mechanism activated by their structural components, such as cellulose, hemicelluloses, and lignin, acting as natural adhesives (Nonaka et al., 2013; Boon et al., 2019). Hot pressing, commonly used in self-bonding, involves temperatures exceeding 170 °C in order to enhance particle interaction (Robles et al., 2016). The chemical reactivity of particles during the hot pressing process has been studied, showing that the lignin components exhibit a high level of reactivity; this leads to the formation of strong bonds and the creation of new materials through processes such as thermal degradation and chemical interaction (Alvarez et al., 2015). Some studies have proposed that the hydrolysis of hemicellulose, as well as the degradation of lignin and cellulose, has developed furfural as a self-bonding agent during the steam or heat treatment (Widyorini et al., 2005a, 2005b). According to Widyorini et al. (2005c), the three main chemical components of lignocellulosic materials and cinnamic acid play a vital role in the self-bonding mechanism of binderless boards. However, appropriate equipment and adequate energy inputs are required for better performance. In addition, the lignocellulosic material's self-bonding mechanism can be formed by hydrogen bonding (Nitu et al., 2019) or polymerization upon heating (Boon et al., 2017), resulting in a reduction in the cost, energy, and hazardous effects of formaldehyde-based adhesives on end users.

Furthermore, research on non-wood lignocellulosic biomass utilization has intensified due to depleted forest resources and environmental concerns (Nonaka et al., 2013; Farrokhpayam et al., 2016). Bagasse, a by-product of sugarcane processing, has been identified as a highly promising raw material for value-added products. Residual sugars in bagasse, which are challenging to treat with conventional adhesives, have led to the suggestion of a hot water pre-treatment method for binderless composite fabrication. Steam injection treatment has been suggested for producing binderless particleboard, showing an effective improvement in self-bonding properties (Xu et al., 2004, 2003; Quintana et al., 2009). However, no study has explored cross-bonded bagasse particleboards, a mechanism that is gaining attention for its potential to enhance mechanical and thermal properties while reducing manufacturing time and energy requirements (Yusof et al., 2019; Jayamani et al., 2020). Thus, this study aimed to produce cross-bonded binderless bagasse boards following the cross-bonding mechanism with pre-treatments of bagasse that do not involve the use of formaldehyde. The study's objectives also included the production of cross-bonded boards using bone glue adhesive and the analysis of the fabricated boards' physical, mechanical, thermal, and chemical properties for comparison with untreated boards. Additionally, this study's distinctive contribution lies in its capacity to augment adhesion strength and longevity, presenting a promising advancement in the manufacturing of environmentally sustainable composite materials for commercial use.

Materials and methods

Raw material preparation

Sugarcane bagasse was collected from a local market in Khulna, Bangladesh. Bone glue was produced in the Wood Products Laboratory, Forestry and Wood Technology Discipline, Khulna University, Bangladesh; it had a pH of 7, a gel time of 2.3 min, and a solid content of 48 %. Each sugarcane was cut to around 30 cm in length. These bagasse particles were boiled in distilled water, then dried in the sun and in an oven at 102 ± 1 °C until the moisture content reached 2–3 %. A portion of the bagasse was not boiled and was used to produce the controlled composites. Table 1 shows the three different pre-treatment conditions of the raw materials.

Manufacturing of cross-bonded bagasse boards

In this study, six types of cross-bonded binderless and bone glue-bonded boards were prepared using treated/untreated bagasse with hot water. Table 2 shows the manufacturing characteristics of each fabricated panel (e.g., material type, treatment type, and process conditions). The processed bagasse particles were hand-formed into homogeneous single-layer mats using a 30 × 30 cm forming box. The mats were formed with 9 layers of bagasse, which were assembled into a cross-alignment with one another, with the expected board thickness being 8 mm. The prepared mats were hot-pressed with 10 MPa pressure at 220 °C for 10 min. At these times, temperature and pressure were fixed by trial and error to produce binderless cross-bonded bagasse composites. The fabricated composites were conditioned at room temperature for 48 h. The density and dimension of the board were 0.8 g/cm^3 and 300 × 300 × 8 mm, respectively. All the samples were stored in a dry place in the laboratory until testing (Fig. 1). Table 2 shows the conditions of mat formation using bagasse to produce composites.

Table 1
Pre-treatment of bagasse for preparing cross-bonded bagasse composites.

Materials type	Boiling time* (min)	Drying conditions	
		Sun dry (day)	Oven dry (h)
Untreated	–	–	–
Treatment 1	30	5	22
Treatment 2	60	5	22

*Bagasse was boiled with distilled water at 100 °C for processing.

Characterization of the fabricated panels

Analysis of physical and mechanical properties

All the analyses were performed according to the Japanese Industrial Standard for particleboards (JIS A 5908, 2003). Samples were conditioned at room temperature with a relative humidity of 60 ± 2 % for 7 days prior to the analysis of the physical properties of the samples, i.e., density, water absorption (WA), and thickness swelling (TS), and the mechanical properties, i.e., modulus of rupture (MOR), modulus of elasticity (MOE), tensile strength, and hardness. The dimensions of the samples for WA and TS were 50 × 50 × 8 mm. All specimens were weighed and measured before soaking in water. After 2 and 24 h of water immersion, WA and TS were determined as short and long-term impact assessments, respectively. The samples were 200 × 50 × 8 mm in dimension for mechanical properties analysis using a Universal Testing Machine (UTM) (SHIMADJU, AG-50 KN, Japan). Three-point bending properties were carried out to determine the MOR and MOE. Each test was performed with at least ten samples as replications.

Fourier transform-infrared spectroscopy (FT-IR) analysis of the samples

The chemical properties and functional units of the prepared cross-bonded bagasse boards were investigated using Fourier Transform Infrared (FTIR) spectroscopy. The infrared spectra of the powder produced from the particleboards were performed using an FTIR spectrometer (PerkinElmer, USA). Each spectrum was recorded in wave number with a 600–4000 cm^{-1} range using the Attenuated Total Reflection (ATR) method coupled with a diamond crystal.

Analysis of thermal properties

To analyze the thermal behavior of the samples, we conducted Thermogravimetric Analysis (TGA) and Derivative Thermogravimetric Analysis (DTG) using differential scanning calorimetry (DSC) (LABSys evo, Setaram Instrumentation, France). The testing was conducted in a nitrogen environment at a heating rate of 10 °C min^{-1}, with temperatures ranging from 25 to 600 °C, following the American Society for Testing and Materials (ASTM E1356) standard.

Statistical analysis

Data analysis was performed using 'RStudio' version 1.1.463 (RStudio Team, 2018). The descriptive statistics (i.e., means, SEs) were calculated using the 'psych' package (Revelle, 2017), while normality and homogeneity were tested with the 'car' package (Fox & Weisberg,

Table 2
Manufacturing conditions of cross-bonded bagasse panels.

Boards Type	Raw materials	Adhesives (12% w/w)	Treatment	Pressing Conditions Pressure (MPa)	Temperature (°C)	Time (min)
T_C	Untreated	–	Hot pressing	10	220	10
T_1	Treatment 1	–	Hot pressing	10	220	10
T_2	Treatment 2	–	Hot pressing	10	220	10
T_3	Untreated	Bone glue	Hot pressing	10	220	10
T_4	Treatment 1	Bone glue	Hot pressing	10	220	10
T_5	Treatment 2	Bone glue	Hot pressing	10	220	10

Fig. 1. (a) Cross-alignment of bagasse in the board matrix; and (b) cross-bonded bagasse panel.

2011). The appropriate transformation was applied to yield normal distributions for all interested traits. An ANOVA model was also involved with the 'car' package at a 5 % significance level (Origin, 2007). All graphs were made with 'ggplot2' (Wickham, 2009).

Results and discussion

Physical properties

The density of the cross-bonded bagasse panels is presented in Fig. 2. The results showed that the densities for binderless panels were 0.72, 0.71, and 0.67 g/cm^3 for Types T_C, T_1, and T_2, respectively, and 0.81, 0.72, and 0.71 g/cm^3 for the bone glue-bonded boards of T_3, T_4, and T_5, respectively. The densities of the bone glue-bonded panels were

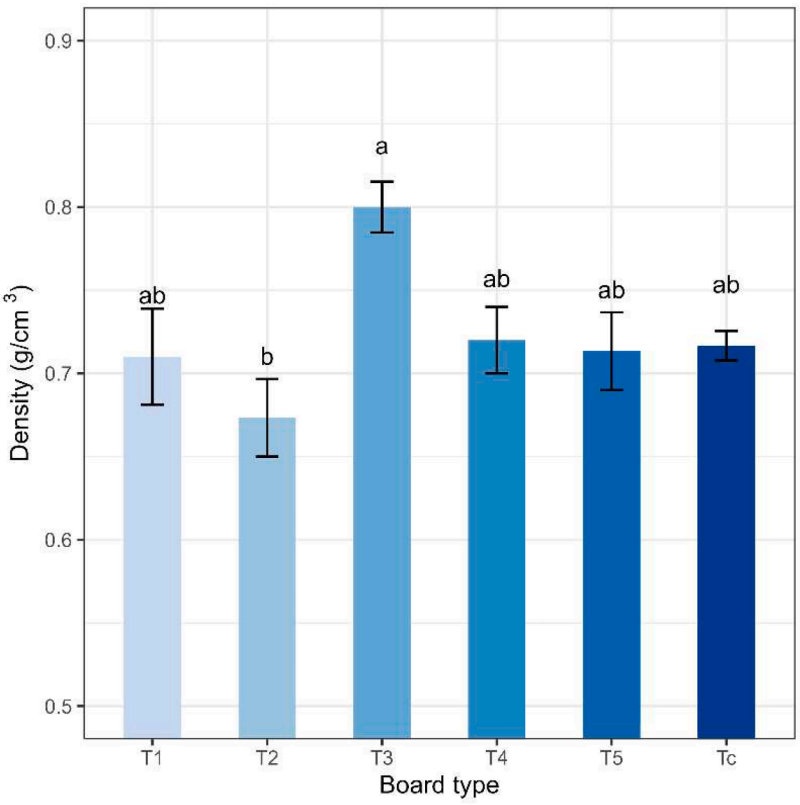

Fig. 2. The density of different types of bagasse panels produced with different pre-treatments and processing conditions.

comparatively higher than those of the binderless panels. The pre-treatment of bagasse particles and their duration reduced the densities of the panels from 0.72 to 0.67 g/cm^3 and 0.81 to 0.71 g/cm^3 for the binderless and bone glue-bonded boards, respectively. T_3-type panels showed the highest density of 0.8 g/cm^3. This might be due to the presence of a free OH (hydroxyl) group in the bagasse particles, which were removed during the boiling of the particles, and also due to the bone adhesive's nature resulting from chemical treatment methods during preparation (Phillips & Williams, 2009). On the other hand, the interconnection between the protein molecules present in bone glue and the OH group of bagasse promotes the formation of bonds within the panel matrix, enhancing particleboard density (Feng et al., 2018). Interestingly, Tc showed a more or less similar result to the panels made of treated particles with bone glue (T_4 and T_5) and without bone glue (T_1). The presence of high OH groups in non-treated particles and the use of a cross-bonding mechanism help to obtain a level of values for the binderless board that is similar to using bone glue-bonded boards. The statistical analysis also confirmed that the density of T_3 was significantly ($p < 0.05$) different from others and that Tc was similar to T_1, T_4, and T_5. Rana et al. (2020) reported that the density of bagasse panels depends on mat compaction, pressing conditions, particle size, raw material density, and binding materials. In this study, pre-treatments, i.e., boiling, might also partially dissolve the soluble materials, including the free sugar molecules and hemicelluloses. Thus, it reduced the particle density, in turn lowering the panel density. Therefore, the boards made from non-boiled particles with bone glue showed the highest panel density.

Water absorption (WA) was measured at 2 and 24 h of immersion in water for the produced panels and is shown in Fig. 3. The T_3 panel type had the lowest WA of 37 and 48 % at 2 and 24 h of immersion in water, respectively, while the T_2 type panel showed the highest WA of 73 and 127 % at 2 and 24 h, respectively. Across the two durations of boiling time, the longer boiling time (60 min) of bagasse particles increased the WA for the binderless panel and reduced it for the bone glue bonded panel when compared to the shorter boiling time (30 min) for both 2 and 24 h of immersion of panels in water. Again, the T_3 panel type showed a similar WA to the Tc panel type. According to the statistical analysis, the WA of the T_3 panel type was not significantly ($p > 0.05$) different from the T_C panel type. Both types showed a lower affinity to water compared to other types of panels. The boiling pre-treatment of bagasse reduces extractives, free sugars, pectin substances, and hemicelluloses from the bagasse. A longer boiling pre-treatment time (60 min) might also reduce the amorphous region of the cellulose and other chemicals, resulting in fewer hydroxyl (OH) groups in the amorphous region of the cellulose polymers and a lower number of extractive materials compared to the shorter boiling pre-treatment time (30 min). Therefore, the WA for the binderless panel (T_2) composed of longer pre-treatment bagasse particles was higher than for other types. However, the opposite behavior was shown for bone-glued bonde boards.

Nevertheless, many hydroxyl groups function as inhibitors for the cohesive forces between particles and facilitate the absorption of moisture by bonding hydrogen with water vapor through the OH groups of sugars (Sulaiman et al., 2012). Consequently, the high content of OH groups that crosslink with bone glue in T_3 and T_C of the panel reduces the WA. Furthermore, the presence of OH groups can provide strong compaction through H-bonding. Thus, comparatively less free space is provided for water uptake; T_3 showed the lowest WA while Tc showed a similar value, which was not significantly ($p > 0.05$) different from T_3. In addition, the presence of extractive content may enhance the inhibition of water uptake in the matrix of the panels. Mendes et al. (2015) observed the WA of bagasse particleboards at 15.7 and 47.1 % for 2 and 24 h, respectively. The WA of T_C and T_3 was higher than in previous studies, as Mendes et al. (2015) used urea-formaldehyde (UF) as an adhesive for bagasse particleboard production. This may be the reason for the lowered WA in the investigation.

The thickness swelling (TS) of the bagasse panels at 2 and 24 h of immersion in water is presented in Fig. 4. As expected, the T_3 type panel showed the lowest TS of 15 and 21 % at 2 and 24 h of immersion in water, respectively, as it had the lowest WA. On the other hand, the T_2 type of panel showed the highest TS values of 66 and 70 % at 2 and 24 h of immersion in water, respectively. In this study, the TS of T_3 was significantly different ($p < 0.05$) from the others. The presence of OH groups in the cellulose polymers results in uptake of water, leading to TS. The existence of many OH groups, on the other hand, prevents water absorption for cohesive force among the particles (Sulaiman et al., 2012). As a consequence, it can reduce the TS of the boards. The boards obtained from non-boiled particles along with bone glue are more likely to have high OH groups and extractives content than other types. In addition, they can provide more bonding sites, enhancing compactness and lowering the free space for water penetration. Therefore, the T_3 board showed the lowest value of TS. In a previous study, the TS of a board produced from bagasse particleboards showed 4.5 and 17.8 % for 2 and 24 h of immersion, respectively (Mendes et al., 2015). The TS was lower than in this current study as the authors used UF as a binding agent, which encapsulates particles and hinders water absorption, resulting in lower TS. Furthermore, the values of TS for T_C and T_3 support JIS A 5908:2003.

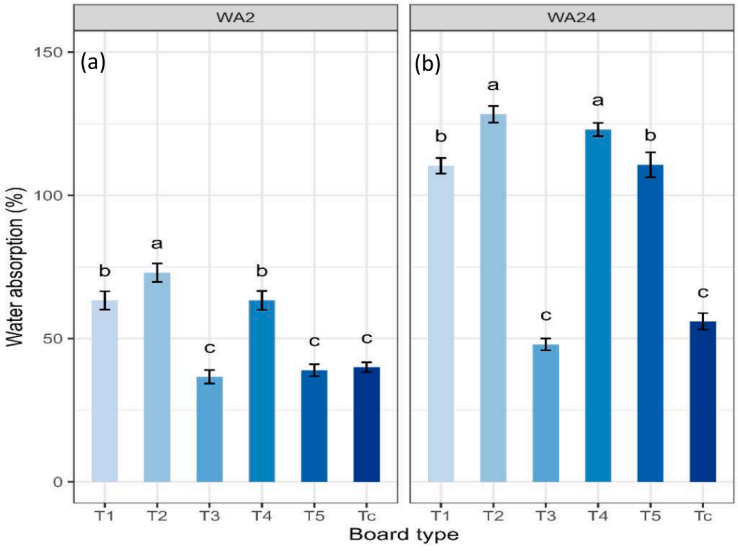

Fig. 3. Water absorption of different types of bagasse panels at 2 h (a) and 24 h (b) of immersion in water.

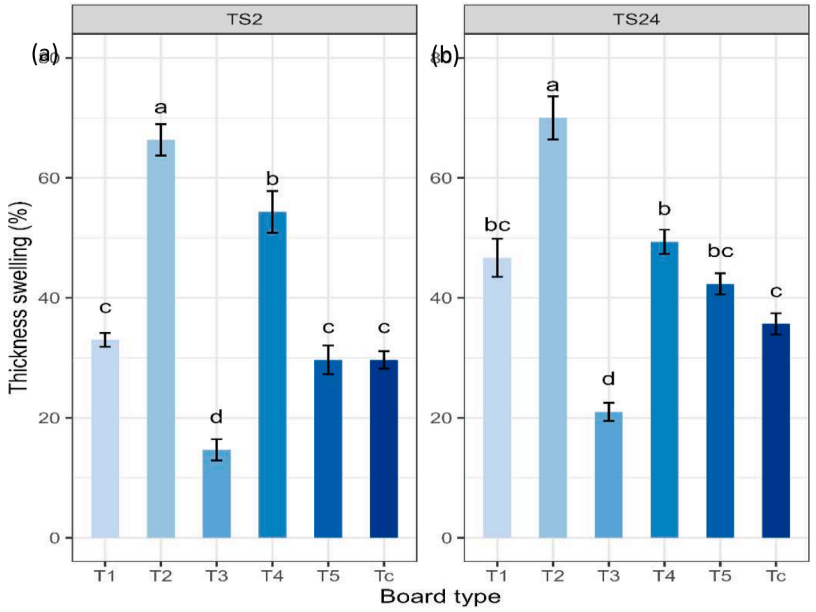

Fig. 4. Thickness swelling of different types of bagasse panels at 2 h (a) and 24 h (b) immersion in water.

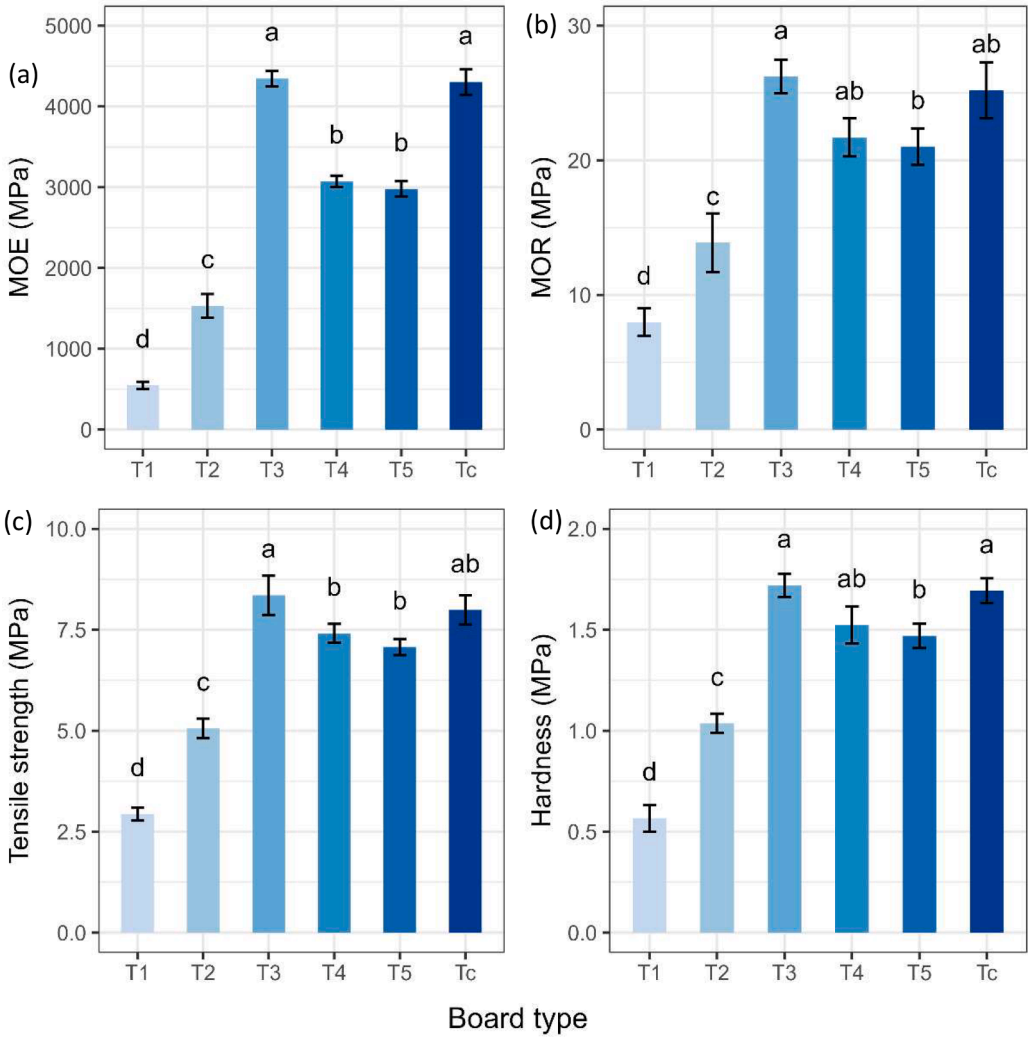

Fig. 5. Mechanical properties of different types of panels made from bagasse - MOE (a), MOR (b), Tensile strength (c), and Hardness (d).

Mechanical properties

The modulus of elasticity (MOE), modulus of rupture (MOR), tensile strength, and hardness of the different types of bagasse panels are depicted in Fig. 5. The T_3 type panel made from untreated bagasse particles using bone glue showed the highest values of MOE (4302 MPa, Fig. 5a), MOR (26.22 MPa, Fig. 5b), tensile strength (8.35 MPa, Fig. 5c), and hardness (1.72 MPa, Fig. 5d). The mechanical properties of T_3 were more or less similar to those of T_C. The mechanical properties of T_3 were significantly different from those of T_1, T_2, T_4, and T_5, while there was no significant difference between T_C and T_3. The mechanical properties of the composite are dependent on the board density, which is correlated proportionally (Rana et al., 2020).

The interfacial adhesion from particle to particle (Kevin et al., 2018) and the crosslinking network between particle and adhesive (Sun et al., 2006) in the composite matrix enhances the compactness, leading to high mechanical properties. The density was highest for T_3, which showed the highest mechanical properties. The density of T_C was close to T_3, and the mechanical properties of T_C were close to those of T_3. Both T_C and T_3 were obtained from untreated bagasse particles. This helped to preserve the chemical component containing OH groups, which might help increase the interfacial bonding between particle-to-particle and cross-linking networks in the board matrix. Thus, it might work as an influential factor in terms of increasing the compactness of the board matrix, leading to higher mechanical properties than the other types. Furthermore, using bone glue for T_3 might enhance compactness more in the matrix compared to T_C and might also result in higher mechanical properties for T_3 than for T_C. Thus, the presence of more OH groups in Tc and the cross-bonding mechanisms enhances more H-bonding compared to other types of boards obtained from treated bagasse particles, leading to greater mechanical properties.

In a previous study, the MOE and MOR of bagasse particleboards were 2095 MPa and 12.5 MPa, respectively, with UF used as an adhesive (Mendes et al., 2015). Astari et al. (2018) found that the MOE and MOR of particleboards obtained from wood particles were around 1200 to 2700 MPa and 11.69 to 26.54 MPa, respectively, where UF and PF were used as adhesives. However, the untreated binderless bagasse panel and the bone glue-based bagasse panel showed higher values of MOE and MOR compared to previous studies. Even the MOE and MOR of both types of panels were in the range of wood particle-based particleboards. In addition, the T_C and T_3 types followed the standards of JIS A 5908:2003, the American National Standards Institute (ANSI A208.1), and the European Standard (EN 312) for mechanical properties, i.e., MOE and MOR.

FTIR analysis of the samples

Sugarcane bagasse, a by-product of the sugarcane industry, is a lignocellulosic material with distinctive composition: around 32–34 % cellulose, 19–24 % hemicellulose, 25–32 % lignin, 6–12 % extractives, and 2–6 % ash. The lignin in sugarcane bagasse is notably enriched with H-type lignin and p-hydroxyphenyl units. During Fourier transform infrared (FT-IR) spectra analysis, specific peaks in the infrared spectrum were identified, providing further insights into the molecular characteristics of this material. The Fourier transform infrared (FT-IR) spectra of the raw, boiled (30 and 60 min) bagasse and the prepared bagasse board types are depicted in Fig. 6. As seen from Fig. 6, raw (R), 30 min boiled (B_{30}), and 60 min boiled (B_{60}) bagasse particles show some characteristic peaks at 3313–3331, 2921, 2327–2337, 1736, 1330–1333, 1243–1250, 1033, 829–833 and 674 cm^{-1}. The broad peak at 3313–3331 cm^{-1} is attributed to the presence of OH groups in the polymeric molecules, e.g., hemicelluloses, simple sugars, celluloses, and lignin of the bagasse, along with the -OH group of moisture (Rodney et al., 2015). The peak at 2921 cm^{-1} is due to C—H stretching vibration (Zia-Ud-Din et al., 2018). The peak at 2327–2337 cm^{-1} is related to free O = C = O groups in the T_1 type of panels. The peak at 1736 cm^{-1} can be

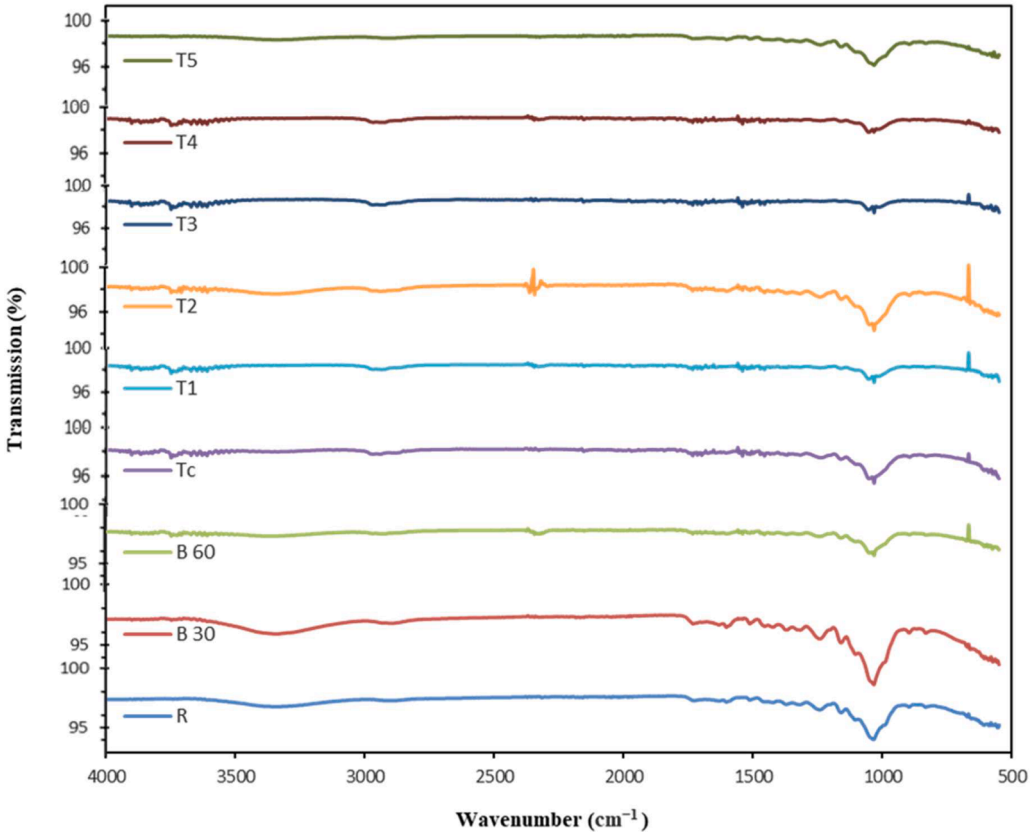

Fig. 6. FTIR spectrum of raw bagasse (R), 30 min boiled bagasse (B_{30}), 60 min boiled bagasse (B_{60}), and prepared bagasse-based panels (T_C, T_1, T_2, T_3, T_4 and T_5).

attributed to the carbonyl group (C = O) in the hemicelluloses and lignin. The intense peak at 1604 cm^{-1} indicates the C = O stretching vibration of aromatic carbonyl compounds. Water molecules adsorb on cellulose, hemicelluloses, and lignin through hydrogen bonding with OH groups. The broad peak at 1330–1333 cm^{-1} represents C—O groups in bagasse. The aryl ether structure peak at 1243–1250 cm^{-1} decreases with increased boiling temperature and time. Peaks at 1033 cm^{-1} arise from OH groups in polysaccharides (Colom et al., 2005; Okuda et al., 2006).

Meanwhile, the untreated and boiled binderless bagasse panels showed a few peaks in their IR spectra (T_C, T_1, and T_2). The peak at 1239–1243 cm^{-1} is derived from an aryl ether structure (Colom et al., 2005), which decreases with increased boiling temperature and time. Okuda et al. (2006) have mentioned that the cleavage of inter-monomer linkages in lignin is due to high temperature and is found in T_1 and T_2 boards. Therefore, a relatively intense peak appears at 1033–1052 cm^{-1} due to the vibration of the C—O single bond for T_C and T_2 bagasse boards. In this study, the panels made with bagasse and bone glue instead showed a few peaks in their IR spectra (T_3, T_4, and T_5). The peak around 3331–3334 cm^{-1} is due to the vibration of OH and NH bonds. The shifting of the peak position from 3331 to 3334 cm^{-1} and the development of hump for types T_3, T_4, and T_5 suggest that bone glue should be incorporated with bagasse particles. As mentioned, the intense peak at 1604 cm-^{1} is due to the -OH bending of the adsorbed water molecules on the bone glue. The type T_3 bone glue-based boards peaked at 1430 cm^{-1} due to the presence of the -CH_2 group. Based on the IR spectral data, it can be concluded that the polymeric polysaccharide molecules were broken down into smaller fragments and monomers by the use of bone glue and boiling pre-treatments. The use of bone glue in the cross-bonded bagasse boards is evident from the appearance of a new peak at 3331–3334 cm^{-1} for the N—H stretching vibration.

Thermal properties of the samples

The thermal evaluation of the samples was carried out in the presence of a standard substance known as alumina. The findings of the study are shown in Fig. 7. The primary distinction between bagasse and the bone glue employed in this investigation is observed before the onset of significant degradation. A notable alteration is observed in all panels' TG and DTG profiles within the temperature range of 70–150 °C. This change corresponds to a minor yet significant deterioration during an endothermic reaction, wherein the absorbed heat is employed. The DTG graph exhibits the variation in weight loss percentage associated with this phenomenon. The TG graph exhibits a slight decrease within the temperature range of 52–122 °C, leading to an approximate weight loss of 5.8 %. This decline suggests the evaporation of moisture present in the structure. However, in bone glue-based boards, the weight loss reaches 5 % and occurs within the temperature range of 80–120 °C. Within the temperature range of 310–357 °C, a notable decomposition occurred, resulting in a subsequent decrease in substance mass. The TG graph reveals a distinct endothermic reaction at around 353 °C, signifying heat absorption. This alteration is attributed to changes in the crystalline region, specifically an increase induced by the boiling of bagasse and the formation of crosslinks with bone glue. The creation of new bonds within the structure also played a role in this transformation. The unanticipated effect on heat absorption underscores the importance of the observed mass reduction. However, the enhancement in crystallinity and the subsequent reformation of certain bonds have contributed to this alteration. The TG graph indicates that the T_3 panel is more stable, thus achieving better results. This may be due to the protein molecules within the amorphous configuration of the bone-derived adhesive exhibiting a notable degree of mobility, allowing for a transformation from a rigid to a pliable and elastic state upon reaching a specific temperature (Islam et al., 2020). Hence, bone glue-bonded bagasse boards, derived from non-boiled particles, displayed higher TG values. The study data reveal that the crosslinking reaction moderately improved the thermal stability of the main components. Additionally, heat application was found to facilitate the crosslinking curing reaction.

Meanwhile, the DTG graph (Fig. 7b) of the samples exhibits a comparable pattern initially, indicating the occurrence of dehydration within the temperature range of 82–130 °C in the composite material, where a weight loss of 4 % was observed. The DTG graph exhibits a comparatively lower rate of weight reduction for the T_3 type of panel. The predominant exothermic breakdown occurred at 290–330 °C. The TG curve clearly shows this reaction, which was caused by the release of volatile gases from polysaccharides (Anannya & Mahmud, 2019). The composite material lost weight, peaking at about 320 °C on the DTG curve. Lignocellulosic materials boosted thermal stability in the composite. Chemical alteration changed the crystalline area and formed new restricted bonds in the T_3 board, improving its thermal stability (Qin et al., 2019). Simultaneously, the incorporation of bone glue alongside lignocellulosic fibrous materials resulted in an enhancement of thermal stability. The findings of this study demonstrate a significant level of thermal resistance in the bagasse boards that were produced.

Conclusion

The production of formaldehyde-free bagasse-based cross-bonded panels is of utmost importance due to its potential to mitigate detrimental environmental and health consequences and to ensure the efficient utilization of raw materials. The cross-bonded bagasse binderless (T_C) and bone glue-bonded (T_3) panels showed superior strength properties compared to the other types of panels. However, the T_C and T_3 bagasse panels showed poor performance in terms of physical properties, i.e., water absorption (WA) and thickness swelling (TS). These panels' mechanical properties, i.e., modulus of rupture (MOR) and MOE, were higher than in previous studies and followed the standards of JIS A 5908:2003, ANSI A208.1, and EN 312. The TS of these panels satisfied

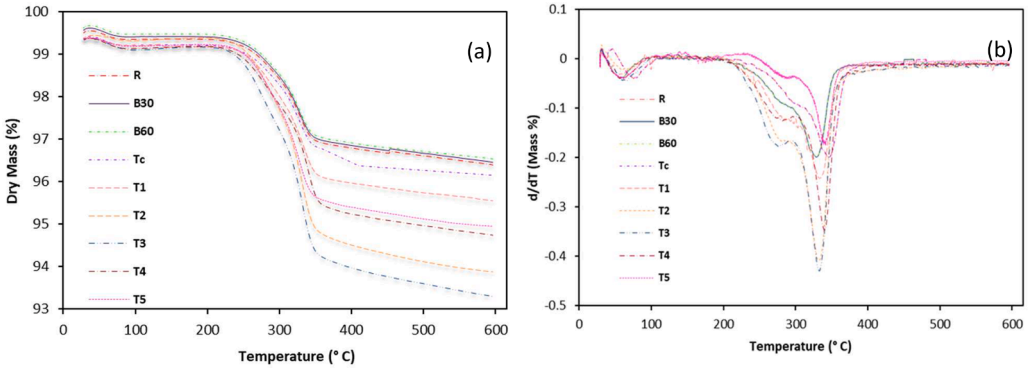

Fig. 7. TG and DTG graphs of raw (R), 30 min boiled (B_{30}), and 60 min boiled (B_{60}) and prepared bagasse-based panels (T_C, T_1, T_2, T_3, T_4 and T_5).

only the JIS A 5908:2003 standard. In addition, T_3 showed better thermal stability than other types. However, the hydrophilic nature of bone-derived adhesives must be addressed in order to meet dimensional stability standards. Further research is needed to overcome water absorption and thickness swelling limitations in cross-bonded bagasse composites, offering a potential avenue for formaldehyde-free bagasse panels.

CRediT authorship contribution statement

Md. Nazrul Islam: Conceptualization, Funding acquisition, Writing – review & editing. **Afroza Akter Liza:** Writing – review & editing, Writing – original draft, Validation. **Moutusi Dey:** Writing – original draft, Formal analysis, Data curation. **Atanu Kumar Das:** Writing – review & editing, Writing – original draft, Validation, Formal analysis. **Md Omar Faruk:** Visualization, Formal analysis, Data curation. **Mst Liza Khatun:** Writing – original draft, Resources, Data curation. **Md Ashaduzzaman:** Writing – review & editing, Methodology. **Xuedong Xi:** Writing – review & editing, Formal analysis.

Declaration of competing interest

No conflict of interest exists.

We wish to confirm that there are no known conflicts of interest associated with this publication and there has been no significant financial support for this work that could have influenced its outcome.

Data availability

Data will be made available on request.

Funding

No funding was received for this work.

Intellectual Property

We confirm that we have given due consideration to the protection of intellectual property associated with this work and that there are no impediments to publication, including the timing of publication, with respect to intellectual property. In so doing we confirm that we have followed the regulations of our institutions concerning intellectual property.

Authorship

The authorship of this article is based on the following four criteria:

Substantial contributions to the conception or design of the work; or the acquisition, analysis, or interpretation of data for the work; AND

Drafting the work or revising it critically for important intellectual content; AND initial approval of the version to be published; AND

Agreement to be accountable for all aspects of the work in ensuring that questions related to the accuracy or integrity of any part of the work are appropriately investigated and resolved.

All those designated as authors should meet all four criteria for authorship, and all who meet the four criteria should be identified as authors.

We confirm that the manuscript has been read and approved by all named authors.

We confirm that the order of authors listed in the manuscript has been approved by all named authors.

Supplementary materials

Supplementary material associated with this article can be found, in the online version, at doi:10.1016/j.carpta.2024.100467.

References

Alvarez, C., Rojas, O. J., Rojano, B., & Ganan, P. (2015). Development of self-bonded fiber- boards from fiber of leaf plantain: Effect of water and organic extractives removal. *Bioresources, 10*(1), 672–683. https://doi.org/10.15376/biores.10.1.672-683

American Society for Testing and Materials. ASTM D-1037. Standard methods of evaluating of wood-base fiber and particles materials. In . *Annual book of ASTM standard Philadelphia*, (2002)). ASTM.

Anannya, F. R., & Mahmud, Md. A. (2019). Developments in flame-retardant bio-composite material production. *Advances in Civil Engineering Materials, 28*(1), 9–22. http://org/10.1520/ACEM20180025.

Astari, L., Prasetiyo, K. W., & Suryanegara, L. (2018). Properties of particleboard made from wood waste with various size. *IOP Conf. Series: Earth and Environmental Science, 166*, Article 012004.

Baharuddin, M. N. M., Zain, N. M., Harun, W. S. W., Roslin, E. N., Ghazali, F. A., & Som, S. N. M. (2023). Development and performance of particleboard from various types of organic waste and adhesives: A review. *International Journal of Adhesion and Adhesives, 124*, Article 103378. https://doi.org/10.1016/j.ijadhadh.2023.103378

Boon, J. G., Hashim, R., Danish, M., & Nadhari, W. N. A. W. (2019). Physical and mechanical properties of binderless particleboard made from steam-pretreated oil palm trunk particles. *Journal of Composites Science, 3*(2), 46. https://doi.org/10.3390/jcs3020046

Boon, J. G., Hashim, R., Sulaiman, O., Sugimoto, T., Sato, M., Salim, N., et al. (2017). Importance of lignin on the properties of binderless particleboard made from oil palm trunk. *ARPN Journal of Engineering and Applied Sciences, 12*(1), 33–40.

Colom, X., & Carrillo, F. (2005). Comparative study of wood samples of the northern area of Catalonia by FTIR. *Journal of Wood Chemistry and Technology, 25*(1–2), 1–11. https://doi.org/10.1081/WCT-200058231

Farrokhpayam, S. R., Valadbeygi, T., & Saneil, E. (2016). Thin particleboard quality: Effect of particle size on the properties of the panel. *Journal of the Indian Academy of Wood Science, 13*(1), 38–43. https://doi.org/10.1007/s13196-016-0163-9

Feng, C., Wang, F., Xu, Z., Sui, H., Fang, Y., Tang, X., et al. (2018). Characterization of soybean protein adhesives modified by xanthan gum. *Coatings, 8*(10), 342. https://doi.org/10.3390/coatings8100342

Ferrandez-Villena, M., Ferrandez-Garcia, C. E., Garcia-Ortuño, T., Ferrandez-Garcia, A., & Ferrandez-Garcia, M. T. (2020). The influence of processing and particle size on binderless particleboards made from Arundo donax L. rhizome. *Polymers, 12*(3), 696. https://doi.org/10.3390/polym12030696

Fox, J., & Weisberg, S. (2011). *An r companion to applied regression* (2nd edn). Thousand Oaks: Sage Publications.

Islam, M. N., Liza, A. A., Farul, M. O., Habib, M., . A.., & Hiziroglu, S (2020). Formulation and characterization of tamarind (Tamarindus indica L.) seed kernel powder (TKP) as green adhesive for lignocellulosic composite industry. *International Journal of Biological Macromolecules, 142*, 879–888. https://doi.org/10.1016/j.ijbiomac.2019.10.027

Islam, M. N., Liza, A. A., Khatun, M. L., Faruk, M. O., Das, A. K., Dey, M., et al. (2021). Formulation and characterization of formaldehyde-free chemically modified bone-based adhesive for lignocellulosic composite products. *Global Challenges, 5*(9), Article 2100002. https://doi.org/10.1002/gch2.202100002

Islam, M. N., Rahman, F., Das, A. K., & Hiziroglu, S. (2022). An overview of different types and potential of bio-based adhesives used for wood products. *International Journal of Adhesion and Adhesives, 112*, Article 102992. https://doi.org/10.1016/j.ijadhadh.2021.102992

Jayamani, E., Rahman, M., Benhur, D. A., Bakri, M. K., Kakar, A., & Khan, A. (2020). Comparative study of fly ash/sugarcane fiber reinforced polymer composites properties. *Bioresources, 15*(3), 5514–5531. https://doi.org/10.15376/biores.15.3.5514-5531

Kevin, E. I., Ochanya, O. M., Olukemi, A. M., Bwanhot, S. T. N., & Uche, I. (2018). Mechanical properties of urea formaldehyde particle board composite. *American Journal of Chemical and Biochemical Engineering, 2*(1), 10–15. https://doi.org/10.11648/j.ajcbe.20180201.12

Liu, Y., Lv, X., Bao, J., Xie, J., Tang, X., Che, J., et al. (2019). Characterization of silane treated and untreated natural cellulosic fibre from corn stalk waste as potential reinforcement in polymer composites. *Carbohydrate Polymers, 218*, 179–187. https://doi.org/10.1016/j.carbpol.2019.04.088

Mendes, R. F., Mendes, L. M., Oliveira, S. L., & Freire, T. P. (2015). Use of sugarcane bagasse for particleboard production. *Key Engineering Materials, 634*, 163–171. https://doi.org/10.4028/www.scientific.net/KEM.634.163

Nitu, I.R., Shams, M.I., Islam, M.N., Ratul, S.B., & Ashaduzzaman, M. (2019). Development of binderless composites from different non-wood lignocellulosic materials: Overview. In L. M. T. Martinez (Eds.), Handbook of ecomaterials, 3, (pp. 1395–1409). Switzerland: Springer International Publishing.

Nonaka, S., Umemura, K., & Kawai, S. (2013). Characterization of bagasse binderless particleboard manufactured in high-temperature range. *Journal of Wood Science, 59*(1), 50–56. https://doi.org/10.1007/s10086-012-1302-6

Okuda, N., Hori, K., & Sato, M. (2006). Chemical changes of kenaf core binderless boards during hot pressing (1): Influence of the pressing temperature condition. *Journal of Wood Science, 52*(3), 244–248. https://doi.org/10.1007/s10086-005-0761-4

Origin. (2007). Northampton, MA: OriginLab.

Phillips, G. O., & Williams, P. A. (2009). *Handbook of hydrocolloids: Second edition* (2nd ed, pp. 1–924). Handbook of Hydrocolloids.

Qin, Y., Zhang, H., Dai, Y., Hou, H., & Dong, H. (2019). Effect of alkali treatment on structure and properties of high amylose corn starch film. *Materials, 12*(10), 1705. https://doi.org/10.3390/ma12101705

Quintana, G., Velasquez, J., Betancourt, S., & Ganan, P. (2009). Binderless fiberboard from steam exploded banana bunch. *Industrial Crops and Products, 29*(1), 60–66. https://doi.org/10.1016/j.indcrop.2008.04.007

Rana, M. N., Islam, M. N., Nath, S. K., Das, A. K., Ashaduzzaman, M., & Shams, M. I. (2020). Influence of chemical additive on the physical and mechanical properties of cement-bonded composite panels made from jute stick. *Journal of Building Engineering, 31*, Article 101358. https://doi.org/10.1016/j.jobe.2020.101358

Revelle, W. (2017). psych: Procedures for psychological, psychometric, and personality research.

Robles, E., Czubak, E., Kowaluk, G., & Labidi, J. (2016). Lignocellulosic-based multilayer self-bonded composites with modified cellulose nanoparticles. *Composites Part B: Engineering, 106*, 300–307. https://doi.org/10.1016/j.compositesb.2016.09.049

Rodney, J., Sahari, J., Kamal, M. S. M., & Sapuan, S. M. (2015). Thermochemical and mechanical properties of tea tree (Melaleuca alternifolia) fibre reinforced tapioca starch composites. *E-Polymers, 15*(6), 401–409. https://doi.org/10.1515/epoly-2015-0074

RStudio Team (2008). RStudio: Integrated Development for R.

Salthammer, T., Mentese, S., & Marutzky, R. (2010). Formaldehyde in the indoor environment. *Chemical reviews, 110*(4), 2536–2572. https://doi.org/10.1021/cr800399g

Sulaiman, N. S., Hashim, R., Amini, M. H. M., Sulaiman, O., & Hiziroglu, S. (2012). Evaluation of the properties of particleboard made using oil palm starch modified with Epichlorohydrin. *Bioresource Technology, 8*, 283–301. https://doi.org/10.15376/biores.8.1.283-301

Sulaiman, N. S., Hashim, R., Sulaiman, O., Nasir, M., Amini, M. H. M., & Hiziroglu, S. (2018). Partial replacement of urea-formaldehyde with modified oil palm starch-based adhesive to fabricate particleboard. *International Journal of Adhesion and Adhesives, 84*, 1–8. https://doi.org/10.1016/j.ijadhadh.2018.02.002

Sun, S., Li, C., Zhang, L., Du, H. L., & Burnell-Gray, J. S. (2006). Interfacial structures and mechanical properties of PVC composites reinforced by $CaCO_3$ with different particle sizes and surface treatments. *Polymer International, 55*, 158–164. https://doi.org/10.1002/pi.1932

Wang, Z., Li, Z., Gu, Z., Hong, Y., & Cheng, L. (2012). Preparation, characterization and properties of starch-based wood adhesive. *Carbohydrate Polymers, 88*(2), 699–706. https://doi.org/10.1016/j.carbpol.2012.01.023

Wickham, H. (2009). *ggplot2: Elegant graphics for data analysis*. New York: Springer.

Widyorini, R., Xu, J., Umemura, K., & Kawai, S. (2005a). Manufacture and properties of binderless particleboard from bagasse I: Effects of raw material type, storage methods, and manufacturing process. *Journal of Wood Science, 51*(6), 648–654. https://doi.org/10.1007/s10086-005-0713-z

Widyorini, R., Xu, J., Watanabe, T., & Kawai, S. (2005b). Chemical changes in steam-pressed kenaf core binderless particleboard. *Journal of Wood Science, 51*, 26–32. https://doi.org/10.1007/s10086-003-0608-9

Widyorini, R., Higashihara, T., Xu, J., Watanabe, T., & Kawai, S. (2005c). Self-bonding characteristics of binderless kenaf core composites. *Wood Science and Technology, 39*, 651–662. https://doi.org/10.1007/s00226-005-0030-0

Vitrone, F., Ramos, D., Ferrando, F., & Salvadó, J. (2021). Binderless fiberboards for sustainable construction. Materials, production methods and applications. *Journal of Building Engineering, 44*, Article 102625. https://doi.org/10.1016/j.jobe.2021.102625

Xu, J., Han, G., Wong, E. D., & Kawai, S. (2003). Development of binderless particleboard from kenaf core using steam-injection pressing. *Journal of Wood Science, 49*, 327–332. https://doi.org/10.1007/s10086-002-0485-7

Xu, J., Sugawara, R., Widyorini, R., Han, G., & Kawai, S. (2004). Manufacture and properties of low-density binderless particleboard from kenaf core. *Journal of Wood Science, 50*, 62–67. https://doi.org/10.1007/s10086-003-0522-1

Yusof, N. M., Md Tahir, P. M., Lee, S. H., Khan, M. S., & James, R. M. S (2019). Mechanical and physical properties of cross-laminated timber made from Acacia mangium wood as function of adhesive types. *Journal of Wood Science, 65*, 20. https://doi.org/10.1186/s10086-019-1799-z

Zhang, D., Zhang, A., & Xue, L. (2015). A review of preparation of binderless fiberboards and its self-bonding mechanism. *Wood Science and Technology, 49*(4), 661–679. https://doi.org/10.1007/s00226-015-0728-6

Zhang, Y. P., Wang, J., Xia, K. W., Zhao, Y. F., Yuan, Q. W., Huang, Z. X., et al. (2023). Water evaporation induced in-situ interfacial compatibilization for all-natural and high-strength straw-fiber/starch composites. *Carbohydrate Polymers, 305*, Article 120535. https://doi.org/10.1016/j.carbpol.2022.120535

Zhou, X., Zheng, F., Lv, C., Tang, L., Wei, K., Liu, X., et al. (2013). Properties of formaldehyde-free environmentally friendly lignocellulosic composites made from poplar fibres and oxygen-plasma-treated enzymatic hydrolysis lignin. *Composites Part B: Engineering, 53*, 369–375. https://doi.org/10.1016/j.compositesb.2013.05.037

Zia-Ud-Din, A., Chen, L., Ullah, I., Wang, P. K., Javaid, A. B., Hu, C., et al. (2018). Synthesis and characterization of starch-g-poly (vinyl acetate-cobutyl acrylate) bio-based adhesive for wood application. *International Journal of Biological Macromolecules, 114*, 1186–1193. https://doi.org/10.1016/j.ijbiomac.2018.03.178